Anesthesiology 2003; 99:1313–22

Setting Mean Airway Pressure during High-frequency Oscillatory Ventilation According to the Static Pressure–Volume Curve in Surfactant-deficient Lung Injury

A Computed Tomography Study

Thomas Luecke, M.D., Juergen P. Meinhardt, M.D.,* Peter Herrmann, Ph.D.,† Gerald Weisser, M.D.,‡ Paolo Pelosi, M.D., Ph.D.,§ Michael Quintel, M.D., Ph.D.‖*

Background: **Numerous studies suggest setting positive end-expiratory pressure during conventional ventilation according to the static pressure–volume (P-V) curve, whereas data on how to adjust mean airway pressure (P_{aw}) during high-frequency oscillatory ventilation (HFOV) are still scarce. The aims of the current study were to (1) examine the respiratory and hemodynamic effects of setting P_{aw} during HFOV according to the static P-V curve, (2) assess the effect of increasing and decreasing P_{aw} on slice volumes and aeration patterns at the lung apex and base using computed tomography, and (3) study the suitability of the P-V curve to set P_{aw} by comparing computed tomography findings during HFOV with those obtained during recording of the static P-V curve at comparable pressures.**

Methods: **Saline lung lavage was performed in seven adult pigs. P-V curves were obtained with computed tomography scanning at each volume step at the lung apex and base. The lower inflection point (Pflex) was determined, and HFOV was started with P_{aw} set at Pflex. The pigs were provided five 1-h cycles of HFOV. P_{aw}, first set at Pflex, was increased to 1.5 times Pflex (termed *1.5 $Pflex_{inc}$*) and 2 Pflex and decreased thereafter to 1.5 times Pflex and Pflex (termed *1.5 $Pflex_{dec}$* and *$Pflex_{dec}$*). Hourly measurements of respiratory and hemodynamic variables as well as computed tomography scans at the apex and base were made.**

Results: **High-frequency oscillatory ventilation at a P_{aw} of 1.5 $Pflex_{inc}$ reestablished preinjury arterial oxygen tension values. Further increase in P_{aw} did not change oxygenation, but it decreased oxygen delivery as a result of decreased cardiac output. No differences in respiratory or hemodynamic variables were observed when comparing HFOV at corresponding P_{aw} during increasing and decreasing P_{aw}. Variation in total slice lung volume (TLV_s) was far less than expected from the static P-V curve. Overdistended lung volume was constant and less than 3% of TLV_s. TLV_s values during HFOV at Pflex, 1.5 $Pflex_{inc}$, and 2 Pflex were significantly greater than TLV_s values at corresponding tracheal pressures on the inflation limb of the static P-V curve and located near the deflation limb. In contrast, TLV_s values during HFOV at decreasing P_{aw} (*i.e.*, 1.5 $Pflex_{dec}$ and $Pflex_{dec}$) were not significantly greater than corresponding TLV on the deflation limb of the static P-V curves. The marked hysteresis observed during static P-V curve recordings was absent during HFOV.**

Conclusions: **High-frequency oscillatory ventilation using P_{aw} set according to a static P-V curve results in effective lung recruitment, and slice lung volumes during HFOV are equal to those from the deflation limb of the static P-V curve at equivalent pressures.**

MECHANICAL ventilation may augment lung injury and contribute to the systemic inflammatory response in patients with acute respiratory distress syndrome (ARDS).[1,2] To avoid ventilator-associated lung injury, current recommendations focus on the avoidance of both alveolar overdistention and alveolar collapse and reexpansion as well as achieving and maintaining alveolar recruitment.[3–5]

High-frequency oscillatory ventilation (HFOV) represents a ventilatory strategy that theoretically achieves all the goals of lung-protective ventilation.[6,7] As discussed by Froese,[6] the ventilating pressure during HFOV should be kept above the lower inflection point, and the peak alveolar pressure should be kept below the upper inflection point on the inflation limb of the pressure–volume (P-V) curve of the respiratory system. Consequently, ventilator-associated lung injury might be attenuated using these boundaries. HFOV oscillates the lung around a constant mean airway pressure (P_{aw}) that is higher than that usually applied during conventional ventilation. Although the oscillations may cause significant proximal and tracheal pressure swings, these pressure fluctuations are significantly attenuated at the alveolar level.[8,9]

Oxygenation during HFOV is primarily affected by P_{aw},[10,11] with the initial setting usually determined by the P_{aw} during conventional ventilation. During the recent Multicenter Oscillatory Ventilation for Acute Respiratory Distress Trial, for example, initial P_{aw} during HFOV was set 5 cm H_2O above P_{aw} during conventional ventilation immediately before conversion to HFOV.[12]

Hypothesizing that a safe range of ventilatory pressures can be predicted from a static P-V relation, aims of the current study were to (1) examine the respiratory and hemodynamic effects of setting P_{aw} during HFOV according to the static P-V curve, (2) assess the effect of increasing and decreasing P_{aw} on slice volumes and aeration patterns at the lung apex and base using computed tomography (CT), and (3) study the suitability of

* Staff Anesthesiologist, † Biomedical Engineer, ‖ Professor, Department of Anesthesiology and Intensive Care Medicine, ‡ Staff Radiologist, Department of Radiology, University Hospital of Mannheim, Faculty of Clinical Medicine Mannheim, University of Heidelberg. § Professor, Department of Clinical and Biological Sciences, University of Insubria.

Received from the Departments of Anesthesiology and Intensive Care Medicine and Radiology, University Hospital of Mannheim, Faculty of Clinical Medicine Mannheim, University of Heidelberg, Mannheim, Germany, and the Department of Clinical and Biological Sciences, University of Insubria, Varese, Italy. Submitted for publication April 14, 2003. Accepted for publication July 30, 2003. Supported in part by a personal research grant from the Faculty of Clinical Medicine Mannheim, University of Heidelberg, Mannheim, Germany (to Dr. Luecke). The high-frequency oscillator was provided by SensorMedics, Yorba Linda, California.

Address reprint requests to Dr. Luecke: Department of Anesthesiology and Intensive Care Medicine, University Hospital of Mannheim, Faculty of Clinical Medicine Mannheim, University of Heidelberg, Theodor-Kutzer Ufer, Mannheim 68167, Germany. Address electronic mail to: thomas.luecke@anaes.ma.uni-heidelberg.de.

the P-V curve to set P_{aw} by comparing CT findings during HFOV with those obtained during recording of the static P-V curve at comparable pressures.

Materials and Methods

Animals and Instrumentation

The study was approved by the Institutional Review Board for the care of animal subjects (University of Heidelberg, Mannheim, Germany). The care and handling was in accord with National Institutes of Health guidelines for ethical animal research. Seven anesthetized domestic pigs (mean weight, 45.9 ± 4.8 kg) were used for the study.

The animals were premedicated with 6 mg/kg azaperone intramuscularly. Anesthesia was induced with 4 mg/kg ketamine intravenously using an ear vein. With the pig breathing spontaneously, a mid-line neck incision was performed. The trachea was isolated and cannulated using a 9-mm-ID cuffed endotracheal jet tube (Hi-Lo Jet®; Mallinckrodt Medical, St. Louis, MO), which provides an additional lumen embedded in the inner wall of the tube. That lumen opens at the carinal end of the tube and was used for tracheal pressure monitoring. After the airway was secured, an additional 3-mg/kg bolus of ketamine along with 6 mg pancuronium was given. Anesthesia and muscle relaxation were maintained by continuous infusion of ketamine ($10\ mg \cdot kg^{-1} \cdot h^{-1}$), midazolam ($1\ mg \cdot kg^{-1} \cdot h^{-1}$), and pancuronium ($0.12\ mg \cdot kg^{-1} \cdot h^{-1}$) throughout the experiment. The animals were placed in a supine position and ventilated with a Siemens Servo Ventilator 300 (Siemens-Elema AB, Solna, Sweden) in the volume-controlled mode with a positive end-expiratory pressure (PEEP) of 5 cm H_2O, an inspiratory:expiratory ratio of 1:2, and a fraction of inspired oxygen (F_{IO_2}) of 1.0. A tidal volume of 12 ml/kg and a respiratory rate of 12–14 breaths/min were applied to maintain an arterial carbon dioxide tension (Pa_{CO_2}) value within the range of 40–50 mmHg. Distal tracheal pressure was measured by connecting an air-filled pressure transducer (Novotrans II; Medex, Hilliard, OH) to the lumen ending at the tip of the tube.

Initially, a continuous infusion of lactated Ringer's solution at a rate of $2\ ml \cdot kg^{-1} \cdot h^{-1}$ was given and increased up to 4 ml/h as indicated by cardiac filling pressures. Gastric emptying was achieved using a large bore orogastric tube, which was removed thereafter.

Central venous and pulmonary artery pressures were measured using a 7.5-French flow-directed thermodilution fiberoptic pulmonary artery catheter (Opticath®; Abbott Laboratories, North Chicago, IL) advanced into the pulmonary artery under transduced pressure guidance *via* the right internal jugular vein. The right carotid artery was cannulated with a 20-gauge catheter (Vygon, Ecouen, France) for blood sampling and arterial pressure monitoring. Continuous electrocardiographic monitoring was performed. For hemodynamic monitoring, a Sirecust 1281 monitor (Siemens Medical Electronics, Danvers, MA) and Novotrans II pressure transducers referenced to atmospheric pressure at the mid-thorax level were used. All hemodynamic and ventilatory variables were recorded in 1-min intervals *via* the digital serial RS-232 interface using the custom-made software package MIDAS (Mannheim Intensive Care Data Acquisition System, developed by our group) based on the graphic programming language G (LabVIEW 6.1®; National Instruments, Austin, TX). Cardiac output was measured in triplicate using the pulmonary artery catheter by injecting 10-ml aliquots of ice-cold saline into the right atrium. Arterial and mixed venous blood gases were analyzed on an ABL300 (Radiometer A/S, Copenhagen, Denmark).

Recording of Static P-V Curves

Before each P-V curve, a recruitment maneuver was performed by inflating the lungs with a pressure of 40 cm H_2O for 15 s to standardize lung volume history and conditions among the animals.

After disconnection from the ventilator for 10 s, allowing complete exhalation to the resting volume of the respiratory system, a calibrated 1.5-l syringe was connected to the endotracheal tube. Static P-V curves were obtained by inflating the lungs in 100-ml increments up to 1,400 ml or until a maximum static pressure of 50 cm H_2O was reached. The lungs were deflated in an identical way immediately thereafter, and the procedure was stopped when a pressure of 0 cm H_2O was reached.

After each volume increment or decrement, a 5-s pause was held to obtain static pressure estimates and to obtain a CT scan at a fixed level at the lung apex or base (see below). During recording of the static P-V curves, all analog pressure signals were filtered, sampled, conditioned, and passed back to a single plug-in board for acquisition directly to the PC memory using a front-end signal conditioning system (SCXI-1000; National Instruments). The analog signals were amplified with a four-channel isolation amplifier with excitation (SCXI-1121), digitized with a multifunction analog–digital converter board (AT-MIO board; sample rate, 300 Hz; resolution, 12 bit), digital filtered with a low-pass Bessel filter (corner frequency, 75 Hz), and stored on hard disk. The pressure and volume signals were recorded and analyzed using the custom-made software package MIDAS (created by Peter Herrmann, Ph.D., Biomedical Engineer, Department of Anesthesiology and Intensive Care Medicine, University Hospital of Mannheim, University of Heidelberg, Mannheim, Germany). The user manually accepted each data point when the pressure signal had reached a quasi–static state level. No corrections for changes in temperature and humidity or oxygen consumption were made for inflation or deflation volume data because of the absence of reliable data for pigs. The lower inflection point (Pflex) was recorded as the pressure at the intersection of the linear extrapolations of the initial and the

most compliant portions of the curve within the tidal volume range.[13,14]

Lung Imaging and Image Analysis

The Imatron C-150XP EBCT scanner (Imatron, San Francisco, CA) was used for the study. Volumetric data sets are acquired with the EBCT scanner by firing electrons at one of four stationary target rings at a rate of 100 ms/sweep together with continuous table motion with up to 30 mm/s. Image reconstruction allows averaging of up to 20 sweeps, resulting in an effective exposure time up to 200 ms (1,240 mA). For CT scanning of the whole lung, the ventilator was switched to the pressure-control mode. The pressure level was set at 40 cm H_2O, and the PEEP level was set at zero. Before each scan, a recruitment maneuver was performed as described above. After an initial scout image, scans of the whole lungs were performed within 14–17 s during end-expiratory hold at zero PEEP and during end-inspiratory hold at 40 cm H_2O (collimation, 3 mm; table feed, 4–5 mm; reconstruction interval, 2–2.5 mm; scan length, 28–35 cm; 130 kV; 128 mA; exposure time, 200 ms/image). For P-V curves and imaging during HFOV, single-slice scanning was performed at two discrete anatomic locations: the lung apex and the lung base. The table locations at these positions were selected from the preceding whole-lung image series during end-expiratory hold, with care taken not to move the animal after the initial scanning. For single-slice scanning after each 100-ml volume step during recording of the P-V curves, the following parameters were used: collimation, 3 mm; 130 kV; exposure time, 100 ms/image. For single-slice scanning during HFOV, the exposure time was extended to 600 ms/image. Because we performed HFOV at a frequency of 4 Hz throughout the study, an "average image" spanning at least two HFOV cycles was obtained. In addition, some scans during HFOV were obtained in the so-called movie mode (a series of 20 images obtained over 2.2 s) to estimate the cycle-induced changes in slice volume compared to the average image. A representative movie-mode sequence and average image are shown in figure 1.

Image Analysis

The original 16-bit cross-sectional DICOM images were processed and analyzed using the custom-made software package MALUNA (Mannheim Lung Analyzing Tool, developed by our group) based on the graphic programming language G (LabVIEW 6.1®, ImaqVision). With manual tracing by eye, the external boundary along the inside of the ribs and the internal boundary along the mediastinal organs and the stomach were drawn for each CT image. All structures not belonging to the lung structure (*i.e.*, mediastinum at the apex and stomach at the lung base) were excluded from further analysis to achieve automated workup. The images were divided into square pixels (size, 0.46 mm^2), and the Hounsfield

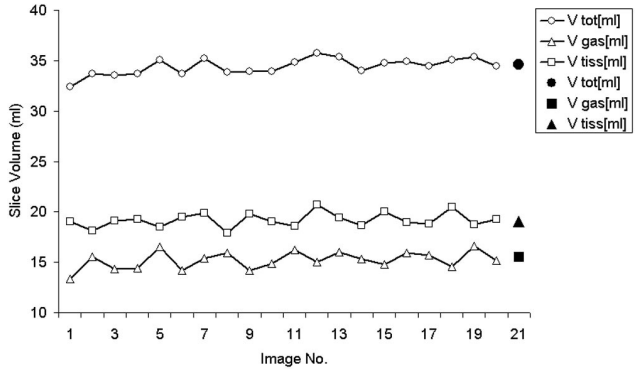

Fig. 1. Slice lung volumes at lung base during high-frequency oscillatory ventilation (mean airway pressure = 1.5 $Pflex_{inc}$) obtained by "movie-mode" scanning (20 images within 2.2 s, 0.1-s scan time). The single *data points* on the right denote the corresponding slice lung volumes obtained during "average" imaging (scan time 0.6 s) used in the study. Vgas = slice gas volume; Vtiss = slice tissue volume; Vtot = total slice lung volume.

attenuation of each pixel was computed. After multiplying the square pixels with the slice thickness, the total lung volume of each slice was divided into voxels (volume, 1.84 mm^3). Voxels were distributed into 100 compartments ranging from −1,000 to + 300 Hounsfield units (HU), with a 13-HU range for each compartment. Absolute lung volumes for each compartment were computed by adding the corresponding voxels. The total lung volume for each slice was obtained by adding the lung volume of each compartment. Because the mean CT number of a given lung volume correlates with the respective proportion of gas and tissue within this lung volume, gas and tissue volumes can be calculated. In the first step, the volume of gas and tissue for each compartment of 13 HU was computed as gas volume = volume × CT/−1,000, and tissue volume = volume × (1 − CT/−1,000), where CT is the mean CT number of the compartment analyzed. In the second step, the volume of gas and volume of tissue for the whole lung were calculated by adding the values of the volumes of gas and the volumes of tissue obtained for each compartment of 13 HU.[15]

To differentiate lung zones with different degrees of aeration, the entire lung was divided into four areas according to Hounsfield unit attenuation: pulmonary parenchyma with densities ranging from −1,000 to −900 HU was classified as overinflated, −900 to −500 HU was classified as normally aerated, −500 to −100 HU was classified as poorly aerated, and −100 to +300 HU was classified as nonaerated (atelectatic).[15]

Experimental Protocol

The pigs were intubated and placed in a supine position in the CT scanner. After instrumentation had been completed and an initial recruitment maneuver had been performed, baseline values were obtained, including arterial and mixed venous blood gases, arterial and pulmonary arterial pressures, central venous pressure, pulmo-

Table 1. Hemodynamic and Respiratory Data at Baseline, after Injury, and during HFOV at Different P_{aw}s

	Baseline	Injury	Pflex	1.5 $Pflex_{inc}$	2 Pflex	1.5 $Pflex_{dec}$	$Pflex_{dec}$
HR, min^{-1}	95 ± 23	113 ± 31	107 ± 25	100 ± 32	102 ± 32	99 ± 25	97 ± 18
MAP, mmHg	76 ± 10	85 ± 28	76 ± 17	67 ± 16	60 ± 10	67 ± 17	76 ± 16
MPAP, mmHg	21 ± 3	35 ± 3*	36 ± 7	39 ± 8*	43 ± 8*†	38 ± 5*	34 ± 8*
CO, l/min	4.6 ± 1.1	6.6 ± 2.1	4.8 ± 1.9	3.4 ± 1.0†	3.1 ± 0.8	3.4 ± 1.0†	4.0 ± 1.4†
Pa_{O_2}, mmHg	497 ± 62	170 ± 94*	335 ± 149	498 ± 104†	563 ± 48†‡§	528 ± 101†‡	375 ± 138
Pa_{CO_2}, mmHg	49 ± 7	72 ± 16*	42 ± 10†	36 ± 7†	35 ± 7†	32 ± 5*†	34 ± 9*†
pH	7.38 ± 0.06	7.20 ± 0.08*	7.41 ± 0.07	7.47 ± 0.08*†	7.49 ± 0.10*†	7.51 ± 0.07*†‡	7.49 ± 0.09*†
Q_s/Q_T	0.14 ± 0.05	0.47 ± 0.21*	0.31 ± 0.17	0.13 ± 0.05†	0.08 ± 0.03†	0.11 ± 0.03†	0.29 ± 0.07
$\dot{D}o_2$, ml/min	693 ± 162	889 ± 293	680 ± 297	507 ± 148†	464 ± 131†	509 ± 148†	580 ± 228
P_{aw}, cm H_2O	7.2 ± 0.4	14.8 ± 1*	20 ± 2.9*†	30.5 ± 4.4*†‡§	40.8 ± 5.9*†‡§‖	30.5 ± 4.4*†‡§	20 ± 2.9*†
OI	1.5 ± 0.2	8.6 ± 5.6*	7.1 ± 3.3*	6.5 ± 2.1*	7.3 ± 1.3*	6.0 ± 1.6*	6.4 ± 3.6*

* $P < 0.01$ *vs.* baseline. † $P < 0.01$ *vs.* injury. ‡ $P < 0.01$ *vs.* $Pflex_{inc}$. § $P < 0.01$ *vs.* $Pflex_{dec}$. ‖ $P < 0.01$ *vs.* 1.5 Pflex (inc and dec).

CO = cardiac output; dec = decrease; $\dot{D}o_2$ = oxygen delivery; Fi_{O_2} = fraction of inspired oxygen; HFOV = high-frequency oscillatory ventilation; HR = heart rate; inc = increase; MAP = mean arterial pressure; MPAP = mean pulmonary artery pressure; OI = oxygenation index, calculated as $P_{aw} \times Fi_{O_2} \times 100/Pa_{O_2}$; Pa_{CO_2} = arterial partial pressure of carbon dioxide; Pa_{O_2} = arterial partial pressure of oxygen; P_{aw} = mean airway pressure; Pflex = inflection point; Q_s/Q_T = transpulmonary shunt.

nary artery wedge pressure, and cardiac output. A static P-V curve was recorded as described above. Lung injury was then produced by bilateral lung lavage. The endotracheal tube was disconnected from the ventilator, and warmed saline was instilled from a height of 50 cm until a meniscus was seen in the tube. The fluid was retrieved *via* gravity drainage after 45 s of apnea followed by endotracheal suctioning. Between the lavages, the pigs were manually ventilated with an Fi_{O_2} of 1 using an AMBU® self-inflating bag (Ambu Inc., Linthicum, MD). The lavage process was repeated until adequate impairment of gas exchange (defined as arterial oxygen tension [Pa_{O_2}] < 200 mmHg, 15 min after the last lavage) was achieved. After lung lavage, lung injury was established by ventilating the pigs with a low end-expiratory pressure of 5 cm H_2O for 60 min.

Thereafter, another set of measurements (injury) was obtained. A recruitment maneuver was performed, and CT scans of the entire lungs were obtained at end expiration (zero end-expiratory pressure) and end inspiration (40 cm H_2O) as described above. Appropriate levels for apex and base scans were identified from the end-expiratory scan and used for single-slice scanning during the P-V curve recordings and during HFOV.

After another recruitment maneuver, a P-V curve along with single-slice scanning at the lung base for each volume step was recorded as described above. Pflex was determined from the tracheal pressure curve. The recruitment maneuver was repeated, and a corresponding P-V curve along with CT scans at the apex of the lung was recorded. Again, Pflex was determined, and the mean value of Pflex was calculated. The pigs were then ventilated with HFOV. Settings of the oscillator (3100B; SensorMedics, Yorba Linda, CA) were as follows: Fi_{O_2}, 1.0; bias flow, 30 l/min; frequency, 4 Hz; pressure amplitude, 60 cm H_2O; inspiratory:expiratory ratio, 1:1. These settings remained unchanged throughout the study unless higher bias flows were necessary to achieve the appropriate P_{aw}. Initially, P_{aw} was set at Pflex. Tracheal pressure readings were used throughout the study to adjust P_{aw}. The pigs were provided with five 1-h cycles of HFOV. P_{aw}, first set at Pflex, was increased to 1.5 times Pflex (termed *1.5 $Pflex_{inc}$*) and 2 Pflex, and decreased thereafter to 1.5 Pflex and Pflex (termed *1.5 $Pflex_{dec}$* and *$Pflex_{dec}$*).

Hourly measurements of arterial and mixed venous blood gases and hemodynamics, as well as CT scans at the apex and base, were made at each P_{aw} studied. After completion of the study, all animals were killed by a bolus dose of thiopental and potassium chloride.

Statistical Analysis

All values are reported as mean ± SD unless otherwise specified. One-way analysis of variance for repeated measurements followed by multiple comparisons (Tukey test) was used to test for differences among baseline conditions, injury, and different levels of P_{aw} during HFOV. Paired *t* tests were used to test for differences between lung volumes before and after injury as well as for differences between slice lung volumes and densities during HFOV and corresponding volume steps during acquisition of the static P-V curve. All statistical tests were used in a descriptive manner. Statistical software package SAS 6.12 (SAS Institute Inc., Cary, NC) was used for analysis, and a *P* value of 0.05 was considered statistically significant.

Results

Lung Injury

The average number of lung lavages needed to establish lung injury was 4 ± 1. Saline lung lavage decreased arterial oxygen partial pressure ($P < 0.01$), increased transpulmonary shunt ($P < 0.01$), and increased P_{aw} ($P < 0.01$). Consequently, the oxygenation index ($OI = P_{aw} \times Fi_{O_2} \times 100/Pa_{O_2}$) increased from 1.5 ± 0.2 to 8.6 ± 5.6 ($P < 0.01$; table 1). Total lung volumes during end-expiratory and end-inspiratory hold are

Table 2. Whole Lung Volumes before and after Injury

	Before Injury		After Injury	
	End-expiration	End-inspiration	End-expiration	End-inspiration
TLV, ml	2,114 ± 184	3,576 ± 242	1,595 ± 122*	2,477 ± 344*
Gas volume, ml	1,443 ± 162	2,901 ± 235	426 ± 58*	1,297 ± 330*
Tissue volume, ml	671 ± 22	675 ± 21	1,168 ± 80*	1,179 ± 71*
Mean CT, HU	−632 ± 36	−811 ± 8	−244 ± 24*	−490 ± 52*
Over, ml	26 ± 17	305 ± 125	4 ± 2	23 ± 20
Norm, ml	1,825 ± 215	3,151 ± 191	254 ± 51*	1,488 ± 621*
Poor, ml	215 ± 33	75 ± 10	989 ± 126*	875 ± 288*
Non, ml	41 ± 6	43 ± 7	349 ± 31*	88 ± 10*

* $P < 0.05$ *vs.* before injury.

CT = computed tomography; End-expiration = end-expiratory hold at zero end-expiratory pressure; end-inspiration = end-inspiratory hold at P_{aw} 40 cm H_2O; HU = Hounsfield unit; non = nonaerated lung volume; norm = normally aerated lung volume; over = overaerated lung volume; poor = poorly aerated lung volume; TLV = total lung volume.

shown in table 2. Saline lung lavage decreased total lung volume and gas volume, whereas lung tissue volume and mean density increased ($P < 0.05$). The changes induced by saline lung lavage are illustrated in figure 2, showing a selection of six CT sections from apex to base at end-expiratory and end-inspiratory hold. Mean P-V curves at baseline and after injury are shown in figure 3. The P-V curve after lung injury revealed a Pflex of 20 ± 2.9 cm H_2O and showed marked hysteresis.

Pulmonary Gas Exchange and Hemodynamics

Baseline and postinjury values during conventional ventilation (PEEP, 5 cm H_2O; F_{IO_2}, 1.0) are shown in table 1. Pa_{CO_2} increased after injury ($P < 0.05$), resulting in moderate acidosis ($P < 0.05$).

With application of HFOV starting at P_{aw} set at Pflex, normocapnia was reestablished and maintained with pressure amplitudes of 60 cm H_2O (table 1). Increasing P_{aw} to 1.5 $Pflex_{inc}$ and 2 Pflex significantly increased the arterial partial oxygen pressure (498 ± 104 mmHg at 1.5 $Pflex_{inc}$, $P < 0.01$ *vs.* after injury, and 563 ± 48 mmHg at 2 Pflex, $P < 0.01$ *vs.* after injury and $Pflex_{inc}$) and decreased venous admixture (Q_S/Q_T) as a result of the decrease in cardiac output (3.4 ± 1.0 l/min at 1.5 $Pflex_{inc}$ and 3.1 ± 0.8 l/min at 2 Pflex *vs.* 6.6 ± 2.1 l/min after injury, $P < 0.01$); however, oxygen delivery also decreased. Doubling P_{aw} significantly increased Pa_{O_2} ($P < 0.01$) but did not improve oxygen delivery. Decreasing P_{aw} from 2 Pflex to 1.5 $Pflex_{dec}$ did not alter gas exchange or hemodynamics. Further decrease in $Pflex_{dec}$ only resulted in a slight decrease in Pa_{O_2} ($P < 0.01$ *vs.* 2 Pflex). No differences in respiratory or hemodynamic variables were observed when comparing HFOV at corresponding airway pressures (*i.e.*, $Pflex_{inc}$ *vs.* $Pflex_{dec}$ and 1.5 $Pflex_{inc}$ *vs.* 1.5 $Pflex_{dec}$).

Lung Volumes at Apex and Base during HFOV

Total lung, air, and tissue volumes at the lung apex and the lung base are shown in table 3. At the lung apex, the total slice lung volume (TLV_s) increased from 8.3 ± 3.1 ml at $Pflex_{inc}$ to 9.4 ± 3.6 ml at 1.5 $Pflex_{inc}$ ($P < 0.01$). Increasing P_{aw} to 2 Pflex further increased TLV_s to 10.3 ± 3.6 ml ($P < 0.01$ *vs* 1.5 $Pflex_{inc}$). Decreasing P_{aw} to 1.5 $Pflex_{dec}$ did not alter TLV_s, whereas further decrease in $Pflex_{dec}$ decreased TLV_s. Of note, TLV_s at $Pflex_{dec}$ was significantly greater than TLV_s at $Pflex_{infl}$ ($P < 0.01$). Because tissue volumes did not change with varying P_{aw}, all changes observed in TLV_s were attributable to parallel changes in gas volume. Radiologic density, expressed as mean Hounsfield units, decreased with increasing P_{aw} ($P < 0.01$) and increased with decreasing P_{aw} ($P < 0.01$ *vs.* 2 Pflex). Mean Hounsfield units were comparable for corresponding levels of P_{aw} during inflation and deflation. Overdistended lung volume was very small and did not change with varying P_{aw}.

At lung base, TLV_s increased from 43.5 ± 7.6 ml at Pflex to 46 ± 8.3 ml at 1.5 $Pflex_{inc}$ ($P < 0.01$). Increasing P_{aw} to 2 Pflex further increased TLV_s to 48.6 ± 8.2 ml ($P < 0.01$ *vs.* 1.5 $Pflex_{inc}$). Decreasing P_{aw} to 1.5 $Pflex_{dec}$ did not alter TLV_s, whereas further decrease to $Pflex_{dec}$ decreased TLV_s ($P < 0.01$). TLV_s at 1.5 $Pflex_{dec}$ was significantly greater than TLV_s at 1.5 $Pflex_{inc}$ ($P < 0.01$), whereas no differences were found for TLV_s at Pflex and $Pflex_{dec}$. Other than at the lung apex, the lung tissue volume decreased with increasing P_{aw} (19.6 ± 2.3 ml at Pflex to 16.4 ± 2.5 ml at 1.5 $Pflex_{inc}$ and 15.5 ± 2 ml at 2 Pflex, $P < 0.01$) and again increased with decreasing P_{aw}. Mean tissue volumes were comparable for corresponding levels of P_{aw} during inflation and deflation. Poorly and nonaerated lung volume significantly decreased (15.4 ± 7.1 ml at Pflex *vs.* 6.2 ± 1.2 ml at 1.5 $Pflex_{inc}$, $P < 0.01$). Further increase to 2 Pflex did not change poorly and nonaerated lung volume. Again, poorly and nonaerated lung volumes, as well as mean Hounsfield units, were comparable for corresponding levels of P_{aw} during inflation and deflation.

Lung Volumes and Mean Radiologic Densities during Static P-V Curves and HFOV

Pressure–slice volume curves for the lung apex and the lung base are shown in figure 4. Corresponding slice volumes obtained during HFOV are shown in table 3.

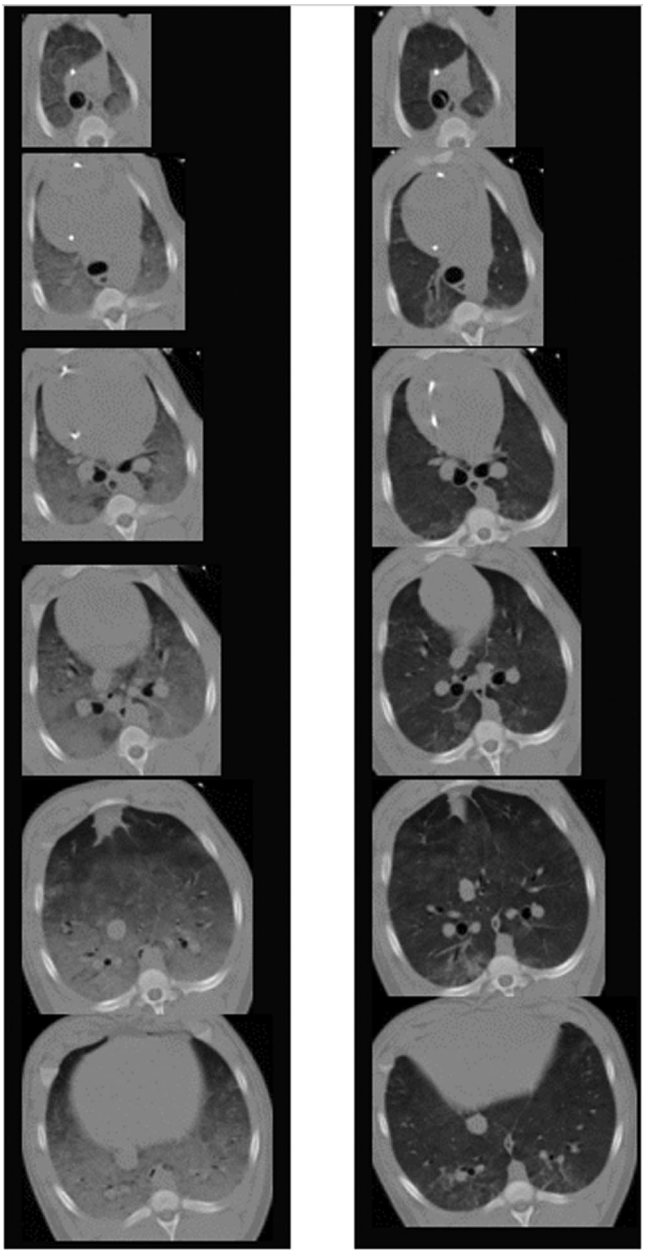

Fig. 2. Selection of computed tomography sections obtained after lung lavage at end-expiratory hold (zero end-expiratory pressure, *left*) and end-inspiratory hold (mean airway pressure = 40 cm H_2O, *right*) in one representative animal showing the diffuse loss of aeration involving all regions including the apex.

Total lung volumes during HFOV at Pflex, 1.5 $Pflex_{inc}$, and 2 Pflex were significantly greater than total lung volumes at corresponding tracheal pressures on the inflation limb of the static P-V curve ($P < 0.05$, paired t tests) and in close proximity to the deflation limb. In contrast, TLV_s values during HFOV at decreasing P_{aw} (*i.e.*, 1.5 $Pflex_{dec}$ and $Pflex_{dec}$) were not significantly greater than corresponding TLV_s values on the deflation limb of the static P-V curves. The marked hysteresis observed during static P-V curve recordings was absent during HFOV.

By plotting the mean Hounsfield units of the slice volumes shown in figure 4 *versus* the resulting tracheal pressure, pressure–density curves were obtained and are shown in figure 5. Except from Pflex at the lung base, the mean Hounsfield units during HFOV at increasing P_{aw} were significantly different from the corresponding values obtained from the inflation limb of the static P-V curves ($P < 0.05$, paired t tests). As for the pressure–slice volume curves, mean Hounsfield units during HFOV at decreasing P_{aw} were not significantly different from the corresponding Hounsfield units on the deflation limb of the static P-V curves. Again, the marked hysteresis observed during static P-V curve recordings was absent during HFOV. As with slice volumes, the mean Hounsfield units during the entire HFOV cycle were in close proximity to the deflation limb of the static P-V curve.

Discussion

The main findings of this study can be summarized as follows: (1) In moderate saline washout–induced lung injury, HFOV using P_{aw} increased and decreased according to the static P-V curve leads to effective lung recruitment. (2) HFOV results in higher lung volume than that of the equivalent pressure on the inflation static P-V curve, and starting HFOV with P_{aw} already set at the lower inflection point already in lung volumes equal to those observed on the deflation limb of the static P-V curve. (3) The marked hysteresis observed on static P-V curves is almost absent during HFOV.

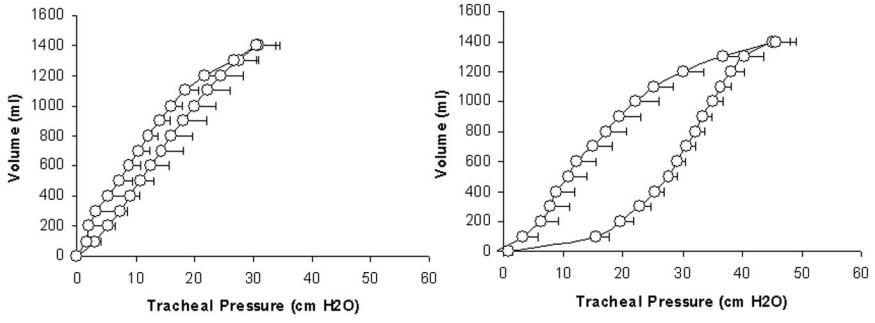

Fig. 3. Static pressure–volume curves before and after injury (mean ± SD).

Table 3. Lung Volumes and Mean CT Numbers at Lung Apex and Base during HFOV at Different P_{aw}s

	Pflex	1.5 $Pflex_{inc}$	2 Pflex	1.5 $Pflex_{dec}$	$Pflex_{dec}$
TLV_s, apex, ml	8.3 ± 3.1	9.4 ± 3.6*	10.3 ± 3.6*†‡	10.0 ± 3.6*‡	9.0 ± 3.3*
Gas volume apex, ml	5.4 ± 2.4	6.6 ± 2.9*‡	7.5 ± 2.9*†‡	7.1 ± 2.9*‡	6.0 ± 2.6*
Tissue volume apex, ml	2.9 ± 1.0	2.8 ± 0.9	2.8 ± 1.0	2.9 ± 1.0	3.0 ± 1.2
Over apex, ml	0.12 ± 0.23	0.21 ± 0.39	0.28 ± 0.45	0.25 ± 0.44	0.12 ± 0.24
Mean HU Apex	−647 ± 79	−699 ± 62*‡	−723 ± 53*‡	−710 ± 61*,‡	−661 ± 80
TLV, base, ml	43.5 ± 7.6	46 ± 8.3*	48.6 ± 8.2*†‡	47.7 ± 7.7*†‡	44 ± 7.6
Gas volume base, ml	23.9 ± 7.2	29.6 ± 6.9*‡	33.2 ± 7*†‡§	31.3 ± 6.4*†,‡	24 ± 6.4
Tissue volume base, ml	19.6 ± 2.3	16.4 ± 2.5*‡	15.5 ± 2*‡	16.5 ± 2.4*‡	20 ± 2.5
Poor/non base, ml	15.4 ± 7.1	6.2 ± 1.2*‡	4.0 ± 0.6*‡	5.0 ± 1.1*‡	14.4 ± 4
Mean HU base	−540 ± 82	−641 ± 47*‡	−682 ± 37*†‡	−655 ± 43*‡	−540 ± 61

* $P < 0.01$ *vs.* $_{inc}$. † $P < 0.01$ *vs.* 1.5_{inc}. ‡ $P < 0.01$ *vs.* $Pflex_{dec}$. § $P < 0.01$ *vs.* 1.5_{dec}.

CT = computed tomography; dec = decrease; HFOV = high-frequency oscillatory ventilation; HU = Hounsfield unit; inc = increase; over = overdistended lung volume; Pflex = inflection point; poor/non = poorly and nonaerated lung volume; TLV = total slice lung volume.

Mean Airway Pressure during HFOV

During HFOV, P_{aw} is the primary variable affecting oxygenation and is set independent of other variables on the oscillator. Because distal airway pressure changes during HFOV are minimal,[8,9] the P_{aw} during HFOV can be viewed in a manner similar to the PEEP level in conventional ventilation.[16] The optimal P_{aw} can be considered as a compromise between maximal lung recruitment and minimal overdistention. To determine lung recruitment, CT is the preferred diagnostic tool, but it is not available at bedside.[17] Therefore, two different strategies have been suggested recently to determine the optimal P_{aw} during HFOV, using the static P-V curve[16] or the OI.[17]

Goddon *et al.*[16] suggested that the P_{aw} that results in optimal oxygenation should be predictable from the P-V curve in a manner similar to that observed in conventional ventilation. During measurement of the P-V curve, it has recently been shown that recruitment occurs throughout inflation,[18–20] reflecting the high opening pressures of many lung units in acute lung injury. The function of PEEP, especially in the surfactant-deficient lung, is to prevent alveolar and small airway pressures from falling below their closing pressures at end expiration, preventing the collapse of units that were inflated at end inspiration.[21] Because significant interrelations have been shown between PEEP and tidal volume in determining recruitment,[19,22] the lack of tidal volume recruitment may be the reason for the postulated need for higher P_{aw} during HFOV to optimize oxygenation.[16] Figure 1 displays an example of the minimal slice volume changes during HFOV with a proximal pressure amplitude of 60 cm H_2O and emphasizes the fact that during HFOV, tidal recruitment as seen during conventional ventilation may be negligible. Goddon *et al.*,[16] also using a saline washout model of lung injury, therefore applied four 1-h cycles of HFOV at different levels of P_{aw} in random order, ranging from Pflex plus 2 cm H_2O to Pflex plus 14 cm H_2O. Each cycle was preceded by a recruitment maneuver at a sustained P_{aw} of 50 cm H_2O for 60 s. The authors found that HFOV with P_{aw} set at Pflex plus 6 cm H_2O resulted in a significant improvement in oxygenation. No further improvement was observed with higher P_{aw}, but cardiac output and oxygen delivery decreased. We used a different strategy to examine the effects of P_{aw} for two reasons. First, we are somewhat concerned about the safety of the recruitment maneuver used in that study and instead favor the approach of a stepwise increase in P_{aw} to open the lung and a stepwise decrease in P_{aw} to keep the lung open. Second, to make sure that recruitment is complete, we used a wider variation in P_{aw} to span the entire range of the static P-V curve, from the lower to the upper inflection point. Because we were somewhat limited in the number of different P_{aw} levels to be tested during HFOV, for technical reasons, we cannot derive a conclusion regarding the optimal P_{aw} because there was a large difference of 10 cm H_2O between the levels of P_{aw} studied. However, bearing these differences and limitations in mind, one can compare our results at least partially with those obtained by Goddon *et al.*[16] Using oxygenation and oxygen delivery as main variables, we could also show that setting P_{aw} above Pflex (*i.e.*, from $Pflex_{inc}$ to Pflex + 10 cm H_2O or 1.5 $Pflex_{inc}$) resulted in improved oxygen-

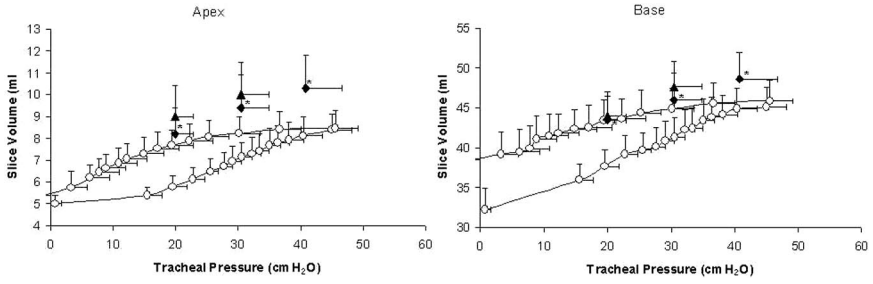

Fig. 4. Pressure–slice volume curves obtained at lung apex and base. Mean slice lung volumes during high-frequency oscillatory ventilation are added (table 3). Note that for reasons of readability, slice volumes are displayed as mean ± SEM. *$P < 0.05$, slice volume during high-frequency oscillatory ventilation *versus* slice volume at the corresponding tracheal pressure level during static pressure–volume recording.

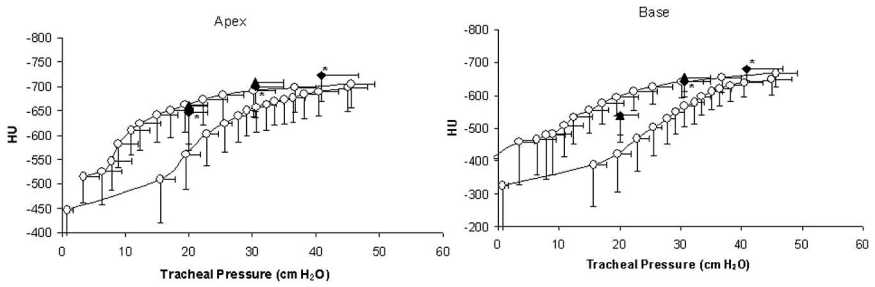

Fig. 5. Pressure–slice density curves obtained at lung apex and base (mean ± SD). Mean slice densities during high-frequency oscillatory ventilation are added (table 3). *$P < 0.05$, mean Hounsfield units (HU) during high-frequency oscillatory ventilation *versus* mean Hounsfield units at the corresponding tracheal pressure level during static pressure–volume recording.

ation. Beyond a critical level of P_{aw} (*i.e.*, at Pflex + 20 cm H_2O or 2 Pflex), no significant improvements in oxygenation were obtained, but cardiac output and oxygen delivery became compromised. However, the design of our study allowed us to take advantage of the marked hysteresis of the P-V curve after injury: We deliberately used the 1-h HFOV at a P_{aw} of 2 Pflex to complete lung recruitment. Because a Q_S/Q_T of less than 0.1 has been used as a marker for a completely recruited lung,[17,23] we probably were able to study the "antiderecruiting" effect[21] of P_{aw} when decreasing P_{aw} from 2 Pflex to 1.5 $Pflex_{dec}$ and $Pflex_{dec}$. Expectedly, decreasing P_{aw} to 1.5 $Pflex_{dec}$ did not alter oxygenation variables, and only a slight decrease in Pao_2 was observed at $Pflex_{dec}$. Aiming at maintaining a completely recruited lung, we would therefore speculate that optimal P_{aw} in our model might be in close proximity to 1.5 $Pflex_{dec}$. Of note, 1.5 $Pflex_{dec}$ is located around the maximal curvature on the deflation limb, confirming the findings by Goddon *et al.*,[16] who also showed that the point of maximal curvature on the deflation limb was equal to the optimal P_{aw} (Pflex + 6 cm H_2O).

Van Genderingen *et al.*[17] used the OI ($OI = P_{aw} \times Fio_2 \times 100/Pao_2$) to identify the optimal P_{aw} during HFOV. The OI has been used to assess the severity of illness in pediatric patients during HFOV[24] and combines the goals to maximize arterial oxygenation and minimize P_{aw} and inspired oxygen concentration. Using saline washout injury in piglets, HFOV was started at P_{aw} set 3 cm H_2O above the mean airway pressure during conventional ventilation and increased in steps of 3 cm H_2O until Pao_2 was more than 450 mmHg. Then, it was lowered accordingly until Pao_2 was less than 80 mmHg. The OI value reached a minimum of 6.2 ± 1.4 at P_{aw} of 30 ± 4 cm H_2O during inflation and a minimum of 2.4 ± 0.3 at P_{aw} of 13 ± 2 cm H_2O during deflation. Although the minimum OI value during inflation was comparable to the values observed in our study (minimum OI value, 6.0 ± 1.6 at 1.5 $Pflex_{dec}$), those authors observed a significantly wider range of OI values (32 ± 10 through 2.4 ± 0.3), a smaller OI value during deflation, and greater differences between inflation and deflation values. However, the reasons for these differences are readily explained. First, the lung injury was apparently more severe than the moderate injury produced in our study. Second, the large tidal volumes (17.1 ± 0.9 ml/kg) used during conventional ventilation in their study may have contributed to the high initial OI value. Third, the smaller OI values during deflation were probably at least partially related to the smaller size of the animals (12 *vs.* 46 kg), resulting in less superimposed pressure due to smaller sternovertebral dimensions. Fourth, and probably most important, the large hysteresis observed in their study is most likely attributable to the short stabilization time (10 min) allowed. Therefore, the authors concluded that longer stabilization times may have resulted in a smaller hysteresis effect because progressive recruitment may have increased oxygenation on the inflation limb and derecruitment may have decreased oxygenation on the deflation limb.[17] The 1-h interval used in our study probably explains the absence of significant differences in oxygenation or OI values at comparable P_{aw} levels during inflation and deflation.

Lung Volumes at Apex and Base during HFOV

Using CT, we were able to analyze the morphologic relations between findings obtained during static P-V recording and dynamic HFOV at comparable tracheal pressures. Unfortunately, scanning of the entire lung during recording of the P-V curve is not feasible; therefore, we limited all analyses to two slices, the lung apex and the lung base. These positions were selected to account at least partially for the steep craniocaudal gradient observed in saline washout–injured lungs, with the lung apex being more prone to overdistention and the lung base showing more severe atelectasis. Making general assumptions on recruitment based on the analysis of a single juxtadiaphragmatic section may be problematic, as shown by Malbouisson *et al.*,[25] who found no correlation between PEEP-induced recruitment and changes in Pao_2, a finding that is most probably a result of the cephalocaudal gradient of recruitment in injured lungs. In addition, imaging at a fixed table position when encountering large ranges of lung volumes can result in imaging a slightly different anatomic lung region during each condition.[26] This problem of displacement has been specifically assessed by comparing the CT slice at HFOV at different P_{aw} levels to the whole-lung studies. Whereas there was virtually no displacement at the lung apex, we found displacement up to 1.2 cm at the lung base over the range of pressures studied. However, the resulting error in volume or density was found to be too small to alter the results obtained (data not shown). As

the degree of displacement was almost identical for comparable pressures during HFOV and P-V recording, differences observed during static P-V recordings and HFOV cannot be attributed to the problem of displacement. Bearing in mind these limitations, we still believe that scanning at two discrete anatomic locations allows some conclusions about volume changes, risk of overdistention, and potential recruitment. Scanning during HFOV at 4 Hz poses some additional problems: Despite the fact that alveolar pressures are known to be small during HFOV and large tidal volume changes observed during conventional ventilation are absent, we aimed at acquiring "comparable" images during different conditions. Therefore, we decided to use "average" images obtained over 0.6 s, thereby spanning at least two HFOV cycles. To validate this approach, we performed additional images in the movie mode; by obtaining 20 images within 2.2 s, we could study cycle-induced volume changes. As displayed in figure 1, cycle-induced changes were small, as expected, and we consider the analysis of average images a valid tool to study lung volume and morphology during HFOV.

Slice lung volumes at the apex and base expectedly increased with increasing P_{aw} and decreased with decreasing P_{aw}. The findings on lung volumes were compatible with those on oxygenation parameters discussed above. Although the high inflation pressures of 40.9 ± 5.9 cm H_2O during P_{aw} of 2 Pflex may raise concerns about potential overinflation, we were not able to show increasing overdistention during increase of P_{aw}. Overall overdistention was less than three percent of TLV at apex and base throughout the study. However, these findings deserve a word of caution: As pointed out by Puybasset *et al.*,[27] the CT attenuation number threshold of −900 HU characterizing lung overdistention was determined in healthy volunteers but may underestimate overdistention in the diseased lung. The spatial resolution of CT is rather low because a voxel contains up to 3,000 alveoli. Therefore, one cannot exclude that a voxel with a CT attenuation greater than −900 HU contains overdistended alveoli in a proportion that could be insufficient to reduce its radiologic density to less than −900 HU. Poorly and nonaerated lung volume significantly decreased beyond Pflex, again emphasizing the concept of ongoing recruitment above the lower inflection point.[18–20] Decreasing P_{aw} from 1.5 $Pflex_{dec}$ to $Pflex_{dec}$ led to a significant increase in poorly and nonaerated lung volume, supporting the finding that optimal P_{aw} in our model may be around 1.5 $Pflex_{dec}$.

Relations between Lung Volumes and Radiologic Density Obtained during Static P-V Curves and during HFOV

The static P-V curves were acquired using the supersyringe technique, which has been largely used to describe the modifications of the elastic properties of the respiratory system related to the severity and stage of ARDS.[28] This method has drawbacks and limitations that have been well described but still represents one of the accepted methods to study P-V relations, especially in the experimental setting.[13] Because no corrections were made to the P-V curve volume data for temperature, humidity, or oxygen consumption, CT slice lung volumes may somewhat underestimate the actual volumes compared to the slice lung volumes during HFOV. Although such corrections may be feasible for the whole-lung P-V curve (fig. 2), it is hardly possible to estimate the corrections necessary for actual slice volumes. The major findings when comparing slice volumes and densities at corresponding pressures during acquisition of static P-V curves and during HFOV are as follows. The marked hysteresis observed during static P-V conditions was almost absent during HFOV, and, during HFOV, volumes and densities were located toward or even beyond the deflation limb of the static P-V curve. The fact that higher lung volumes were obtained during HFOV than during static P-V recording at similar levels of airway pressure may be related to different causes. First, it cannot be ruled out that even measuring airway pressure at the distal end of the endotracheal tube may underestimate the true alveolar pressure because of differences in inspiratory and expiratory resistance and differences in pressure transmission to the distal lung through the complex branching pattern of the tracheobronchial tree.[29] Second, HFOV may normalize the P-V curve by reopening the entire lung, as shown in a previous study on saline-lavaged rabbits.[30] In addition, and probably most importantly, the time scale for the static P-V curve (around 2 min) and the HFOV P-V curve (5 h) were totally different. Therefore, time-dependent reopening of collapsed lung regions during the HFOV period may have normalized the static P-V curve. Starting HFOV at Pflex and ventilating the lung for 1 h already resulted in slice lung volumes that were not expected from the static P-V relation and might indicate progressive recruitment over time as described above. The minimization of hysteresis observed during further changes in P_{aw} may be due to the fact that after 60 min, Pflex was already close to open-lung P_{aw}.[31] Whether tidal recruitment during HFOV also contributed to results observed remains questionable. Although Sedeek *et al.*[32] reported delivered tidal volumes of up to 4.4 ml/kg using identical HFOV settings in saline-lavaged sheep, we tend to be cautious in using those data to predict tidal volumes in our study for various reasons, such as difference in species and size (29 *vs.* 46 kg) of the animals and lack of gas exchange data given in that study. Based on the "dynamic" CT data obtained in this study, we would tend not believe that tidal recruitment was responsible for the results observed. The precise mechanisms remaining questionable, it has to be concluded that the "recruiting effect" of HFOV set at Pflex and applied to the lung for

a sufficient amount of time is largely underestimated by the static P-V curve.

Limitations

The major limitation of this study is that it was performed on a saline washout injury model of ARDS and not in patients. ARDS in patients is rarely, if ever, solely a result of surfactant deficiency,[15] and alveolar flooding rather than lung collapse is the predominating mechanism of the loss of aeration. In this setting, there may be less or no collapse and PEEP may reestablish lung aeration by displacing the gas fluid interface at the alveolar level.[33] As a result, the response of the ARDS lung may be very different from that of the saline washout–injured lung, and the relation between volumes and aeration patterns at comparable tracheal pressures during static P-V analysis and HFOV may be different. Limiting CT analysis to two discrete anatomic positions must be considered as another drawback of this study as discussed above. The different time scales for the static P-V curve and the HFOV P-V curve also pose a limitation on this study because time-dependent reopening of collapsed lung regions during the HFOV period may have normalized the static P-V curve. However, that problem is inherent to each strategy using a P-V relation to adjust ventilator settings.

In the light of these limitations, the major findings of this study can be summarized as follows: (1) HFOV using P_{aw} set according to the static P-V curve leads to effective and safe lung recruitment. (2) HFOV results in higher lung volume than that of the equivalent pressure on the inflation static P-V curve, and starting HFOV with P_{aw} already set at the lower inflection point already in lung volumes equal to those observed on the deflation limb of the static P-V curve. (3) The marked hysteresis observed on static P-V curves is almost absent during HFOV.

References

1. Ranieri VM, Suter PM, Tortorella C, De Tullio R, Dayer JM, Brienza A, Bruno F, Slutsky AS: Effect of mechanical ventilation on inflammatory mediators in patients with acute respiratory distress syndrome: A randomized controlled trial. JAMA 1999; 282:54–61
2. Chiumello D, Pristine G, Slutsky AS: Mechanical ventilation affects local and systemic cytokines in an animal model of acute respiratory distress syndrome. Am J Respir Crit Care 1999; 160:109–16
3. Ware LB, Matthay MA: Medical progress: The acute respiratory distress syndrome. N Engl J Med 2000; 342:1334–49
4. Hudson LD: Protective ventilation for patients with acute respiratory distress syndrome. N Engl J Med 1998; 338:385–7
5. Marini JJ: Recruitment maneuvers to achieve an "open lung": Whether and how? Crit Care Med 2001; 29:1647–8
6. Froese AB: High-frequency oscillatory ventilation for adult respiratory distress syndrome: Let's get it right this time! Crit Care Med 1997; 25:906–8
7. Krishnan JA, Brower RG: High-frequency oscillatory ventilation for acute lung injury and ARDS. Chest 2000; 118:795–807
8. Gerstmann DR, Fouke JM, Winter DC, Taylor AF, deLemos RA: Proximal, tracheal and alveolar pressures during high-frequency oscillatory ventilation in a normal rabbit model. Pediatr Res 1990; 28:367–73
9. Pillow JJ, Neil H, Wilkinson MH, Ramsden CA: Effect of I/E ratio on mean alveolar pressure during high-frequency oscillatory ventilation. J Appl Physiol 1999; 87:407–14
10. Bond DM, Froese AB: Volume recruitment maneuvers are less deleterious than persistent low lung volumes in the atelectasis-prone rabbit during high-frequency oscillatory ventilation. Crit Care Med 1993; 21.402–12
11. Froese AB, McCulloch PR, Sugiura M, Vaclavik S, Possmayer F, Moller F: Optimizing alveolar expansion prolongs the effectiveness of exogenous surfactant therapy in adult rabbits. Am J Respir Crit Care Med 1993; 148:569–77
12. Derdak S, Mehta S, Stewart TE, Smith T, Rogers M, Buchman TG, Carlin B, Lowson S, Granton J, Multicenter Oscillatory Ventilation for Acute Respiratory Distress Syndrome Trial (MOAT) Study Investigators: High-frequency oscillatory ventilation for acute respiratory distress syndrome in adults: A randomized, controlled trial. Am J Respir Crit Care Med 2002; 166:801–8
13. Maggiore SM, Brochard L: Pressure-volume curve in the critically ill. Curr Opin Crit Care 2000; 6:1–10
14. Slinger PD, Kruger M, McRae, Winton T: Relation of the static compliance curve and positive end-expiratory pressure on oxygenation during one-lung ventilation. ANESTHESIOLOGY 2001; 95:1096–102
15. Vieira SRR, Puybasset L, Lu Q, Richecoeur J, Cluzel P, Coriat P, Rouby JJ: A scanographic assessment of pulmonary morphology in acute lung injury. Am J Respir Crit Care 1999; 159:1612–23
16. Goddon S, Fujino Y, Hromi JM, Kacmarek RM: Optimal mean airway pressure during high-frequency oscillation. ANESTHESIOLOGY 2001; 94:862–9
17. Van Genderingen HR, Van Vught JA, Jansen JCR, Jansen JR, Duval EL, Markhor DG, Versprille A: Oxygenation index, an indicator of optimal distending pressure during high-frequency oscillatory ventilation? Int Care Med 2002; 28: 1151–6
18. Crotti S, Mascheroni D, Caironi P, Pelosi P, Ronzoni G, Mondino M, Marini JJ, Gattinoni L: Recruitment and derecruitment during acute respiratory failure: A clinical study. Am J Respir Crit Care Med 2001; 164:131–40
19. Hickling K: Recruitment greatly alters the pressure volume curve: A mathematical model of ARDS lungs. Am J Respir Crit Care Med 1998; 158:194–202
20. Jonson B, Richard JC, Straus C, Mancebo J, Lemaire F, Brochard L: Pressure-volume curves and compliance in acute lung injury: Evidence of recruitment above the lower inflection point. Am J Respir Crit Care Med 1999; 159:1172–8
21. Hickling K: Low tidal volume ventilation: A PEEP at the mechanisms of derecruitment. Crit Care Med 2003; 31:318–9
22. Richard JC, Brochard L, Vandelet P, Brenton L, Maggiore SM, Jonson B, Clabault K, Leroy J, Bonmarchand G: Respective effects of end-expiratory and end-inspiratory pressures on alveolar recruitment in acute lung injury. Crit Care Med 2003; 31:89–92
23. Boehm SH, Vazques de Anda GF, Lachmann B: The open lung concept, Yearbook of Intensive Care and Emergency Medicine 1998. Edited by Vincent J-L. Berlin, Germany, Springer, 1999, pp 430–40
24. Arnold JH, Hanson JH, Toro-Figuero LO, Gutierrez J, Berens RJ, Anglin DL: Prospective, randomized comparison of high-frequency oscillatory ventilation and conventional ventilation in pediatric respiratory failure. Crit Care Med 1994; 22:1530–9
25. Malbouisson LM, Muller JC, Constantin JM, Lu Q, Puybasset L, Rouby JJ, CT Scan ARDS Study Group: Computed tomography assessment of positive end-expiratory pressure-induced alveolar recruitment in patients with acute respiratory distress syndrome. Am J Respir Crit Care Med 2001; 163:1444–50
26. Marcucci C, Nyhan D, Simon BA: Distribution of pulmonary ventilation using Xe-enhanced computed tomography in prone and supine dogs. J Appl Physiol 2001; 90:421–30
27. Puybasset L, Guzman P, Muller JC, Cluzel P, Coriat P, Rouby JJ: Regional distribution of gas and tissue in acute respiratory distress syndrome: I. Consequences for the effects of positive end-expiratory pressure Int Care Med 2000; 26:1215–27
28. Matamis D, Lemaire F, Harf A, Brun-Buisson C, Ansquer JC, Atlan G: Total respiratory pressure-volume curves in the adult respiratory distress syndrome. Chest 1984; 86:58–66
29. Pillow JJ, Sly PD, Hantos Z, Bates JHT: Dependence of intrapulmonary pressure amplitudes on respiratory mechanics during high-frequency oscillatory ventilation in preterm lambs. Pediatr Res 2002; 52:538–44
30. Bond DM, McAloon J, Froese AB: Sustained inflations improve respiratory compliance during high-frequency oscillatory ventilation but not during large tidal volume positive-pressure ventilation in rabbits. Crit Care Med 1994; 22: 1269–77
31. Hickling KG: Best compliance during a decremental, but not incremental, positive end-expiratory pressure trial is related to open-lung positive end-expiratory pressure: A mathematical model of acute respiratory distress syndrome lungs. Am J Respir Crit Care Med 2000; 163:69–78
32. Sedeek KA, Takeuchi M, Suchodolski K, Kacmarek RM: Determinants of tidal volume during high-frequency oscillation. Crit Care Med 2003; 31:227–31
33. Hubmayr RD: Perspective on lung injury and recruitment: A skeptical look at the opening and collapse story. Am J Respir Crit Care Med 2002; 165:1647–53